Journal of Power Sources 190 (2009) 592–595

Contents lists available at ScienceDirect

Journal of Power Sources

journal homepage: www.elsevier.com/locate/jpowsour

Short communication

New, low-cost, high-power poly(*o*-anisidine-*co*-metanilic acid)/activated carbon electrode for electrochemical supercapacitors

D. Kalpana[a,c], Y.S. Lee[a,b,*], Y. Sato[d]

[a] The Research Institute for Catalysis, Chonnam National University, Gwangju 500-757, Republic of Korea
[b] The Faculty of Applied Chemical Engineering, Chonnam National University, Gwangju 500-757, Republic of Korea
[c] Central Electrochemical Research Institute, Karaikudi 630 006, India
[d] Department of Applied Chemistry, Kanagawa University, 3-27-1 Rokkakubashi, Kanagawa-ku, Yokohama 221-8686, Japan

ARTICLE INFO

Article history:
Received 14 November 2008
Received in revised form
29 December 2008
Accepted 13 January 2009
Available online 30 January 2009

Keywords:
Conducting polymer
Poly(*o*-anisidine-*co*-metanilic acid)
Potentiodynamic: activated carbon
Supercapacitor
Cyclic voltammetry

ABSTRACT

A poly(*o*-anisidine-*co*-metanilic acid)/activated carbon composite is evaluated as an active material for electrochemical supercapacitors. Poly(*o*-anisidine-*co*-metanilic acid) (PASM) is potentiodynamically deposited on an activated carbon (AC)-coated stainless-steel substrate, in a supporting electrolyte of 1.0 M H_2SO_4 containing dissolved *o*-anisidine and metanilic acid, at a sweep rate of 50 mV s^{-1}. Scanning electron micrographs show a uniformly deposited, thick PASM film on the activated carbon. Electrochemical techniques, such as impedance analysis, cyclic voltammetry and galvanostatic experiments, are carried out to investigate the suitability of the PASM/AC electrode for supercapacitor applications. A maximum specific capacitance of 576 F g^{-1} is obtained for PASM/AC at a 5 mA cm^{-2} current density.

1. Introduction

Supercapacitors have recently become a frontier area of research given the significant enhancement of their power densities. Among the several materials studied for capacitor applications, such as high surface-area carbon and metal oxides like hydrous RuO_2, conducting polymer-based materials offer advantages in terms of preparation, low cost, excellent reversibility, and high capacitance [1–3]. The π-conjugated double-bonds in the backbone of the conducting polymers transfer electrical charge from the current-collector to the electrolyte [4]. Polymers such as polyaniline, polythiophene and polypyrrole have been reported [5–9] with polyaniline and its derivatives having distinct advantages as the chemically flexible NH-group in the polymer backbone do not take part in protonation and de-protonation, but rather contribute to π-bond formation to ensure sound environmental stability [10].

Self-doped conducting polymers are of considerable interest due to their unique electroactive properties. In the case of polyaniline, self-doped polymers are synthesized by introducing sulfonic acid groups ($-SO_3^-$) into the polymer backbone through electrocopolymerization techniques. These negatively-charged groups act as intramolecular dopant anions that are able to compensate positive charges at protonated nitrogen atoms of the polymer backbone, thus replacing auxiliary dopant anions. The inner anion doping determines many distinctive properties of self-doped polyaniline (PANI), which differs from those of the parent polyaniline [11]. In this work, poly(*o*-anisidine) is selected as one monomer of the aniline family due to its higher solution processability [12]. Studies related to the copolymerization of anisidine are limited and its compatibility with metanilic acid is expected to yield a product different from aniline. Moreover, the known solubility of polyanisidine promotes coupling with this metanilic acid for copolymer synthesis. Thermodynamically, electrodeposition of the conducting polymer on oxidizable metal is a difficult process as the metal dissolves before the electropolymerization potential of the monomer is reached. Hence, it is important to find electrochemical conditions that lead to partial passivation of the metal and decrease its dissolution rate in order to achieve deposition of a conducting polymer on oxidizable metals. Therefore, poly(*o*-anisidine-*co*-metanilic acid) is deposited on activated carbon-coated stainless-steel to avoid dissolution of the deposition. The same method has been used for electrodes in supercapacitors.

To the best of our knowledge, there are few reports in the literature of poly(*o*-anisidine-*co*-metanilic acid) (PASM)/activated carbon (AC) composites as an electrode material for electrochemical capacitors. The objectives of this communication are: (i) the

* Corresponding author at: Faculty of Applied Chemical Engineering, Chonnam National University, Gwang-ju 500-757, Korea. Tel.: +82 62 530 1904; fax: +82 62 530 1909.
E-mail address: leeys@chonnam.ac.kr (Y.S. Lee).

0378-7753/$ – see front matter © 2009 Elsevier B.V. All rights reserved.
doi:10.1016/j.jpowsour.2009.01.056

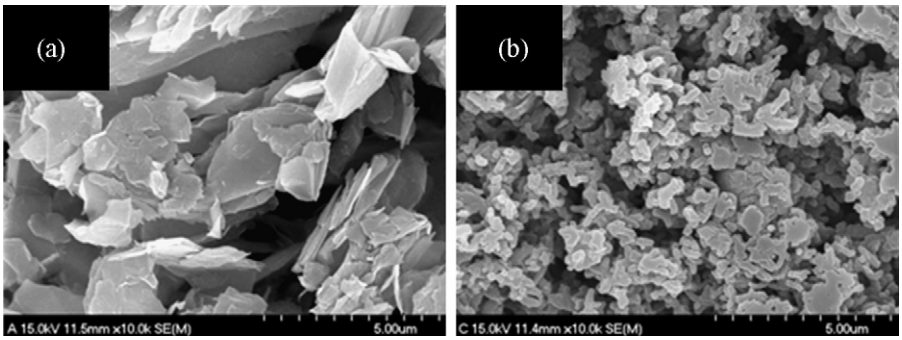

Fig. 1. SEM images of: (a) activated carbon; (b) PASM on activated carbon.

use low-cost, common, stainless-steel metallic substrates for potentiodynamic electrodeposition of PASM; (ii) characterization of the surface morphology by SEM; (iii) comparison of the electrochemical properties of AC, PASM, and PASM/AC by cyclic voltammetry; (iv) evaluation of the cycling performance of a PASM/AC electrode in 0.1 M H_2SO_4.

2. Experimental

O-Anisidine was distilled prior to use. The *o*-anisidine and metanilic acid copolymer were deposited on stainless-steel that was coated with activated carbon. The activated carbon electrode was prepared by mixing 70 wt.% AC (specific surface area of 700 $m^2\ g^{-1}$), 25 wt.% acetylene black and 5 wt.% *N*-methylpyrrolidine binder. The mixture was pressed on a stainless-steel grid current-collector (geometrical area = 1 cm^2) and kept in an oven at 200 °C for 30 min. A glass cell, which was fitted with a ground glass joint suitable for the introduction of the working electrode, was employed along with platinum foil as the counter electrode and an SCE (saturated calomel electrode) as the reference electrode. Polymerization was carried out in a supporting electrolyte of 1.0 M H_2SO_4 that contained dissolved *o*-anisidine and metanilic acid in a 3:1 mole concentration of 0.1 M. Growth of the PASM was carried out at room temperature by a potentiodynamic method.

In the potentiodynamic method, the electrode was subjected to cycling between −0.2 and 0.8 V, and the growth of the copolymer deposit to the required thickness was achieved by cycling 100–200 sweep rates at 50 mV s^{-1}. Potentiodynamic copolymer deposition was carried out using a computer-controlled BAS 100B electrochemical analyzer. Electrochemical half-cell measurements were conducted on a 3-electrode cell equipped with an SCE reference electrode, a Pt counter electrode and a PASM/carbon composite electrode as the working electrode. Capacitor performance was characterized by means of cyclic voltammetry (100B, BAS Electrochemical Analyzer, USA), a.c. impedance measurements in the frequency range of 100 kHz to 10 Hz (6310, EG&G Princeton Applied Research), and galvanostatic charge–discharge cycling at a constant current density of 5 mA cm^{-2} (3000, Won-A-Tech Automatic Battery Cycler, Korea). The deposited copolymer was scrapped off to examine its morphology by field emission scanning electron microscopy (S-4700, Hitachi, Japan). The possible reaction taking place during the electrochemical oxidation of *o*-anisidine

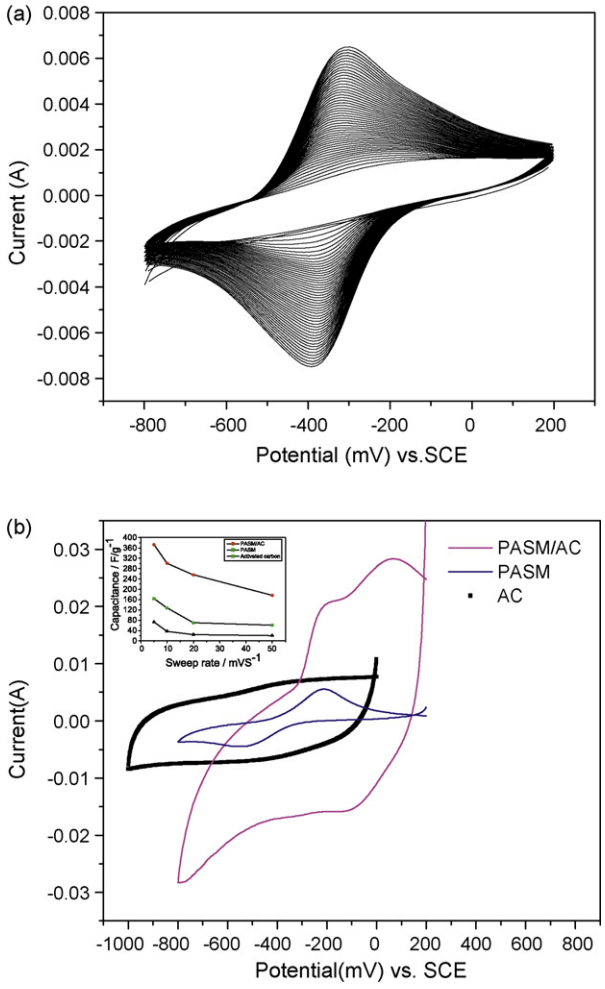

Fig. 2. (a) Cyclic voltammogram recorded during electrodeposition of PASM on activated carbon-coated SS substrate. (b) CV of AC, PASM/SS, and PASM/AC electrodes in 0.1 M H_2SO_4 with respect to SCE recorded at 5 mV s^{-1}.

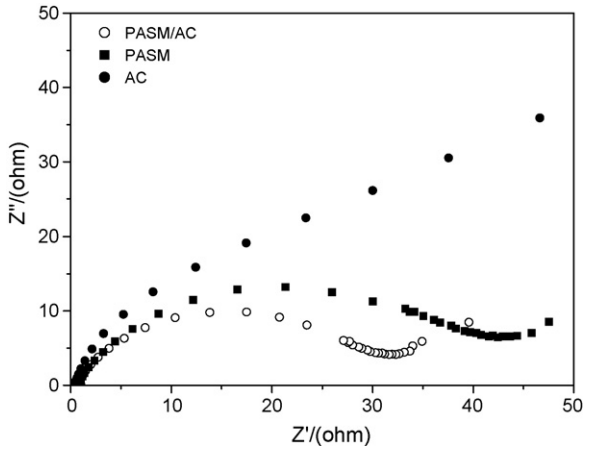

Fig. 3. Typical Nyquist impedance plot of AC, PASM, and PASM/AC electrodes at 0 V potential.

and metanilic acid in aqueous, acidic electrolyte to produce the copolymer is given by:

$$xC_6H_4(SO_3H)NH_2 + yC_6H_4(OCH_3)NH_2$$
$$\rightarrow (C_6H_3(SO_3H)NH-)_x - (C_6H_3(OCH_3)NH-)_y -$$
$$+ 2(x+y)H^+ + 2(x+y)e^-$$

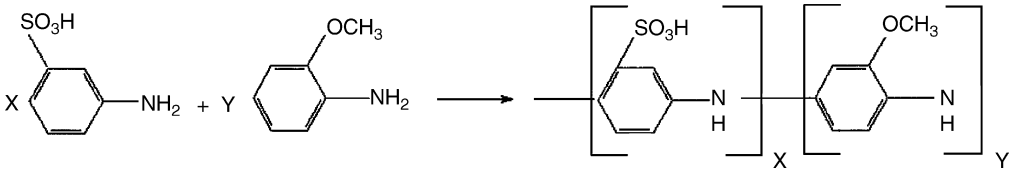

3. Results and discussion

The powder morphology of the AC and PASM/AC composite was investigated by means of SEM; the images are shown in Fig. 1. The surface morphology of the activated carbon (Fig. 1(a)) is relatively smooth and is completely coated with PASM (Fig. 1(b)) when the number of growth cycles increases. The PASM layer has a thickness of about 10 μm and is composed of many small particles with sizes between 50 and 100 nm. The PASM/AC composite also has a particle morphology capable of providing a high-surface area and hence an enhanced electrical conductivity. High porosity was suggested as a key parameter for obtaining high power densities [13]. It is also expected that the electropolymerization of PASM on activated carbon with an adequate particle size (100 nm) is crucial as an ideal electrode candidate for supercapacitor applications to achieve high power density at a high current density.

Fig. 2(a) shows the cyclic voltammogram recorded during electrodeposition of PASM on an AC-coated stainless-steel substrate. The growth and formation of the polymer film can be easily seen from the increase in intensity of the oxidation and reduction peaks. A comparison of the CVs for AC, PASM/SS and PASM/AC recorded at a 5 mV s^{-1} scan rate with respect to SCE in 0.1 M H_2SO_4 is given in Fig. 2(b). The voltammograms of the AC electrode are nearly rectangular in shape without diffusion-controlled current peaks. There is only one redox peak observed for the PASM/SS electrodes due to a leucoemaraldine-to-emaraldine transition. According to a previous report [14], a fresh nucleation in each cycle is likely to produce a discontinuous phase that results in a porous deposit. As expected, the growth of the deposit takes place layer by layer, with each layer becoming electrochemically active before the next layer is deposited. Hence, PASM deposited on activated carbon by potentiodynamic methods is more effectively activated since the polymerization is uninterrupted.

The CV response of PASM/AC shows the features of capacitive behaviour synchronizing both double-layer and redox capacitive features. These redox transitions occur simultaneously with the exchange of ions, and this compensates the excess charge within the polymer. The current of both anodic and cathodic half-cycles is larger than AC and PASM. Hence, PASM/AC electrodes are expected to perform better than AC and PASM electrodes in supercapacitor applications. A specific capacitance of 373 F g^{-1} at a power density of 0.22 kW kg^{-1} is obtained for PASM/AC at a 5 mV s^{-1} scan rate. The value of capacitance is higher than the individual electrodes, which is attributed to the combined effect of the double-layer and redox capacitive behaviour as seen in cyclic voltammogram.

Fig. 3 shows typical Nyquist impedance plots for AC, PASM, and PASM/AC electrodes at 0 V potential. A distorted semicircle in the high-frequency region, due to porosity of the PASM deposition, and a vertical linear spike are observed. The high-frequency intercept on the real axis provides the ohmic resistance (R_Ω) and the diameter of the semicircle gives the charge-transfer resistance (Rct) at the PASM|electrolyte interface. The value of R_Ω is 0.08, 0.71 and 0.18 Ω for the AS, PASM and PASM/AC electrodes, respectively. As evident from the diameter of the semicircles, the Rct value increases for PASM, but not for the PASM/AC electrode. This is due to the transformation of active emaraldine to the leucoemaraldine state [15]. In the PASM/AC spectrum, the angle made by the low-frequency data is low (~45°) compared with the PASM electrode, proving that the system behaves as an ideal capacitor. The Warburg behaviour seen in the spectrum is due to the diffusion-controlled doping–dedoping of anions. PASM and PASM/AC electrodes behave almost identically in the high-frequency region but the PASM/AC composite exhibits more capacitance compared with PASM, as evidenced in the low-frequency region.

Generally, the electrodeposited coating may undergo rapid pulverization during charge–discharge cycles due to the thickness and instability of the coating. When deposited on high surface-area carbon, however, the polymer film will grow layer by layer and there will be an adhesive force between the polymer film and the activated carbon. Additionally, the small particle size of the PASM may reduce the pulverization and hence enhance the electrochemical behaviour upon cycling. This can be measured in this study with great ease.

To find the practical feasibility of the PASM, galvanostatic charge–discharge cycle tests were conducted on symmetric

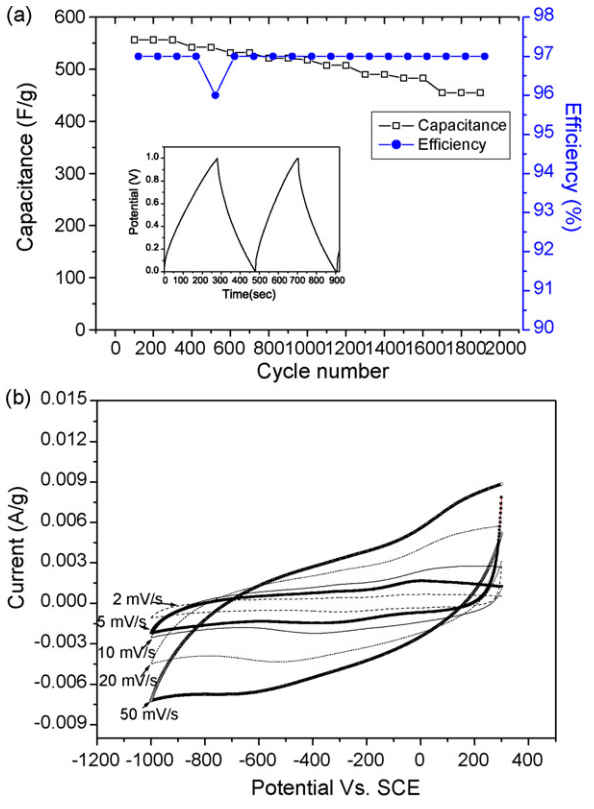

Fig. 4. (a) Capacitance and columbic efficiency with number of cycles. Inset shows galvanostatic charge–discharge curves of PASM/SS electrode at a 5 mA cm^{-2} current density. (b) Cyclic voltammograms of PASM/AC electrode recorded at 2, 5, 10, 20 and 50 mV s^{-1} scan rates after 2000 cycles.

PASM/AC electrodes at a 5 mA cm^{-2} current density over a potential window of 1 V for up to 2000 cycles. The inset in Fig. 4(a) shows that the charging curves are symmetric and that they correspond to the discharging curves indicative of the capacitive behaviour of the PASM/AC electrode. The voltage variation is also linear during both charging and discharging. The positive potential was maintained at a value no greater than 1 V and thus the negative potential limit should not fall below 0 V, preventing oxidative degradation of the polymer film and a subsequent decrease in capacitance [16]. As evident from Fig. 4(a), the ohmic drop is minimum, and the inset proves the stability of the electrode material. A maximum specific capacitance as high as 576 F g^{-1} is obtained for the symmetric PASM/AC capacitor with the specific capacitance of the symmetric type electrochemical capacitor, based on potentiodynamically-deposited PASM, almost constant up to 2000 cycles at a columbic efficiency of nearly 98%, as shown in Fig. 4(a).

Cyclic voltammograms (Fig. 4(b)) of the PASM/AC electrode recorded at 2, 5, 10, 20, and 50 mV s^{-1} scan rates after 2000 cycles show acceptable reversible behaviour. The exact explanation for the effect of sweep rate of PANI deposition on specific capacitance is not clearly given by any author. From the SEM, CV, EIS and charge–discharge cycle tests, however, it is proposed that the growth of a uniform and thicker layer of PASM on high surface area-activated carbon prevents solubility of the polymer film in acidic solutions and hence increases conductivity.

4. Conclusion

The practical feasibility of potentiodynamically-deposited PASM on activated carbon-coated stainless steel is demonstrated for supercapacitor applications. Electron micrographs show that the PASM on activated carbon has a smooth and uniform particle morphology. The a.c. impedance studies reveal that the capacitance value increases at low frequencies, while cyclic voltammetric data from the PASM/AC electrode indicates a specific capacitance of 373 F g^{-1} at a 5 mV s^{-1} scan rate. Charge–discharge curves show a minimal IR drop up to 2000 cycles with a columbic efficiency of approximately 98%. This novel system yields as high a specific capacitance of 576 F g^{-1} at 5 mA cm^{-2} current density. This study will give new insights into the use of PASM/AC composites as a potential electrode material for supercapacitor applications.

Acknowledgement

One of the authors, D. Kalpana, is grateful to Prof. A.K. Shukla, Director, CECRI, and CSIR for granting leave to undertake a post-doctoral fellowship at Chonnam National University, South Korea. This work was supported by the Korea Research Foundation Grant funded by the Korean Government (MOEHRD) (KRF-2007-412-J02003).

References

[1] B.E. Conway, Electrochemical Supercapacitors: Scientific Fundamentals and Technological Applications, Kluwer Academic Plenum Publishers, New York, 1999.
[2] S. Sarangapani, B.V. Tilak, C.P. Chen, J. Electrochem. Soc. 143 (1996) 3791–3799.
[3] J.P. Zheng, T.R. Jow, J. Power Sources 62 (1996) 155–159.
[4] Y. Shen, M. Wan, Synth. Met. 96 (1998) 127–132.
[5] A. Rudge, I. Raistrick, S. Gottesfeld, J.P. Ferraris, Electrochim. Acta 39 (1994) 273–287.
[6] B. Muthulakshmi, D. Kalpana, N.G. Renganathan, S. Pitchumani, J. Power Sources 158 (2006) 1533–1537.
[7] C.C. Hu, C.H. Chu, J. Electroanal. Chem. 503 (2001) 105–116.
[8] P. Rajakumar, D. Kalpana, N.G. Renganathan, S. Pitchumani, Synth. Met. 157 (2007) 899–904.
[9] B. Wessling, Synth. Met. 93 (1998) 143–154.
[10] A.F. Diaz, J.A. Logan, J. Electroanal. Chem. 111 (1980) 111–114.
[11] J. Yue, A.J. Epstein, Z. Zhong, P.K. Gallogher, A.G. MacDiarmid, Synth. Met. 41 (1991) 765–768.
[12] P. Rajakumar, D. Kalpana, N.G. Renganathan, S. Pitchumani, J. Electrochim. Acta 54 (2008) 442–447.
[13] B.E. Conway, J. Electrochem. Soc. 138 (1991) 1539–1548.
[14] K. Rajendra Prasad, N. Munichndraiah, J. Electrochem. Soc. 149 (2002) A1393–A1399.
[15] D.E. Stilwell, S.M. Park, J. Electrochem. Soc. 135 (1988) 2254–2261.
[16] T.C. Girija, M.V. Sangaranarayanan, Synth. Met. 156 (2006) 244–250.